CrossMark

Solar wind implantation into lunar regolith: Hydrogen retention in a surface with defects

W.M. Farrell [a,c,*], D.M. Hurley [b,c], M.I. Zimmerman [b,c]

[a] NASA/Goddard Space Flight Center, Greenbelt, MD 20771, United States
[b] Johns Hopkins University/Applied Physics Laboratory, Laurel, MD 20723, United States
[c] NASA's Solar System Exploration Research Virtual Institute, NASA/Ames Research Center, Moffett Field, CA 94035, United States

ABSTRACT

Solar wind protons are implanted directly into the top 100 nm of the lunar near-surface region, but can either quickly diffuse out of the surface or be retained, depending upon surface temperature and the activation energy, U, associated with the implantation site. In this work, we explore the distribution of activation energies upon implantation and the associated hydrogen-retention times; this for comparison with recent observation of OH on the lunar surface. We apply a Monte Carlo approach: for simulated solar wind protons at a given local time, we assume a distribution of U values with a central peak, U_c and width, U_w, and derive the fraction retained for long periods in the near-surface. We find that surfaces characterized by a distribution with predominantly large values of U (>1 eV) like that expected at defect sites will retain implanted H (to likely form OH). Surfaces with the distribution predominantly at small values of U (<0.2 eV) will quickly diffuse away implanted H. However, surfaces with a large portion of activation energies between 0.3 eV < U < 0.9 eV will tend to be H-retentive in cool conditions but transform into H-emissive surfaces when warmed (as when the surface rotates into local noon). These mid-range activation energies give rise to a diurnal effect with diffusive loss of H at noontime.
Published by Elsevier Inc. This is an open access article under the CC BY-NC-ND license (http://creativecommons.org/licenses/by-nc-nd/3.0/).

1. Introduction

The year 2009 was a very exciting time for lunar research, with two major findings regarding water at the Moon: the first finding was the Lunar Crater Observation Sensing Satellite (LCROSS) observation of copious amounts of water and ice released from the floor of polar crater Cabeus; this observation made immediately following the purposeful impact of a Centaur booster stage (Colaprete et al., 2010; Schultz et al., 2010). The second finding was the discovery of an OH veneer extending from the poles to equator; this remote-sensed by its 3 μm IR spectral absorption feature detected by instruments onboard Chandraayan-1, EPOXI, and Cassini (Pieters et al., 2009; Sunshine et al., 2009; Clark, 2009).

While there had been past tantalizing evidence for water present in permanently shadowed craters (Watson et al., 1961, 1963; Arnold, 1979; Lanzerotti et al., 1981; Feldman et al., 1998), the observation of OH in surficial middle and low latitude regolith at 10–1000 ppm (Clark, 2009) was considered surprising given past Apollo sample analysis (a thorough discussion was presented in McCord et al. (2011)). An added feature of this veneer was the possible reduction in surficial OH as regions rotated into warmer local noon, suggesting a possible diurnal effect (Sunshine et al., 2009). This dynamic aspect pointed to a possible exogenic solar wind source for hydroxylation (Zeller et al., 1966; Pieters et al., 2009; Sunshine et al., 2009).

McCord et al. (2011) examined the possible sources of this veneer, including intrinsic mineralogy, cometary and meteoric infall, and solar wind proton/regolith interaction, and concluded that the complex array of sources, especially feldspathic mineralogy and solar wind implantation, are likely acting simultaneously to account for the hydroxyl IR absorption. Water transport from polar craters to mid-latitudes (liberated by impact vaporization and sputtering) was found to be plausible but could not account for the relatively large hydroxylation levels observed in the IR (Farrell et al., 2013). Kramer et al. (2011) found that the local IR OH absorption feature was reduced (less OH content) in swirl regions associated with magnetic anomalies. The finding suggests that hydroxylation is locally reduced where the B-field also blocks solar wind propagation onto the surface (Kramer et al., 2011; Poppe et al., 2012).

In this paper, we will perform an investigation of the solar wind implantation process, expanding the fundamental work on the subject originally presented by Starukhina (2001, 2006, 2012).

These past works considered the possibility that implantation, H-trapping at defect sites, and OH formation was possibly occurring in cold lunar polar craters and on cool asteroids. The presentation herein is an examination of the implantation and H-loitering process which can be applied to the IR-detected, spatially-extended OH veneer as well.

2. Implantation of protons into oxygen-rich regolith

The solar wind protons and electrons flow out from the Sun at speeds nominally near 400 km/s. The density at 1 AU is typically 5 ions/cm^3 containing ~95% proton, 2–4% He^{++}, and the remainder made up of trace species of heavier ions (like O^{7+}) (Killen et al., 2012). However, the solar wind has variability: During impulsive coronal mass ejections (CMEs), the speed can become in excess of twice the nominal values, the density can be a factor of 10 times larger than nominal values, and the relative concentration of heavy ions (He^{++}, O^{7+}, etc.) can increase to beyond 20%. For airless bodies like the Moon, the dayside surfaces are directly exposed to this fast streaming plasma while nightside/shadowed surfaces are in a relative plasma void. In the void regions, plasma concentrations are at 1/500 of that in the nominal solar wind (Halekas et al., 2005; Farrell et al., 2008).

Fig. 1 shows possible pathways for the incident solar wind protons. Recent observations suggest that about 1% of the incoming protons are reflected back into the solar wind (Saito et al., 2008), but this reflected ion component can increase to close to 50% over magnetic anomalies (Lue et al., 2011; Poppe et al., 2012). Incoming protons should charge exchange with the surface (Hodges, 2011) and observation suggests that about 20% of the incoming solar wind is re-emitted as low energy neutral H (McComas et al., 2009; Futaana et al., 2012). However, some fraction of the incoming protons may implant and 'react' (at defect sites, etc.) with oxygen atoms in the oxide-rich regolith to form exogenically created surficial OH (as discussed by Zeller et al. (1966) and more recently by Pieters et al. (2009), Sunshine et al. (2009), McCord et al. (2011)). We will examine this particular implantation scenario.

Starukhina (2001, 2006, 2012) examined solar wind proton implantation even prior to the discovery of the extended OH veneer in 2009; this for explaining the possible build up of H in cold trap regions of craters and on cold asteroids. As described in these foundation-level works, 1 keV solar wind protons will

undergo charge exchange with the surface neutrals (see also Hodges (2011)) and implant as H in the first 100 nm of regolith material. However, their diffusion time, τ_D, back out into free space is a strong function of surface temperature and number of 'trapping' defects (i.e., crystal lattice vacancies) (Starukhina, 2006, 2012; Dyar et al., 2010). The ability of a region in a crystal to locally trap a free hydrogen is represented by the activation energy, U, with large values of U (>1 eV) representative of locations where the H is locally trapped and would have difficulty migrating away. In contrast, low values of U that may be associated with a mostly-uniform crystal lattice or with a vertical channel defect lead to fast H diffusion even at relatively low temperatures. As such, the surface concentration (1/m^2), σ, of Hs is (Starukhina, 2001)

$$\sigma = F_{sw}h^2/D = F_{sw}\tau_D \qquad (1)$$

where F_{sw} is the solar wind flux (in units of 1/m^2 s), h is the ~100 nm implantation depth, and D is the diffusion coefficient, $D = D_o \exp(-U/kT)$. Thus, the diffusion time (or H 'loitering' or H retention time) is

$$\tau_D = h^2 \exp(U/kT)/D_o \qquad (2)$$

Fig. 2 shows a family of diffusion time curves, each with the same D_o (=10^{-6} m^2/s (Starukhina, 2001)) and temperature range, but having differing activation energies, U. We also identify a lunation at 28 days or 3 × 10^6 s (horizontal line). In examining Fig. 2, we note the following:

(1) Over the temperature range applicable to the equatorial lunar surface, the H diffusion (retention) times span many orders of magnitude. For example, for U = 0.5 eV, the diffusion time varies from 10^{-2} s in warm regions to 10^{15} s in cold (near-terminator) regions.

(2) In the lower left hand side, the curve of U = 0.2 eV corresponds to either a defect-free region of the crystal or one with a vertical 'channel' defect (Starukhina, 2001). In this case, the crystal very quickly diffuses any incident protons back into free space, on time scales of <30 s. We can think of this surface as an 'H-emitting' surface, since any incident proton returns back into space as H (McComas et al., 2009; Futaana et al., 2012) or H$_2$ (Starukhina, 2006).

(3) In the upper right side, the curve of U = 1.2 eV corresponds to a region in the lattice with a vacancy or hole-type defect. Any H in this crystal will have difficulties migrating, with diffusion times greatly exceeding 3 × 10^6 s (a month) even in the warmest locations. In this case, we can consider the
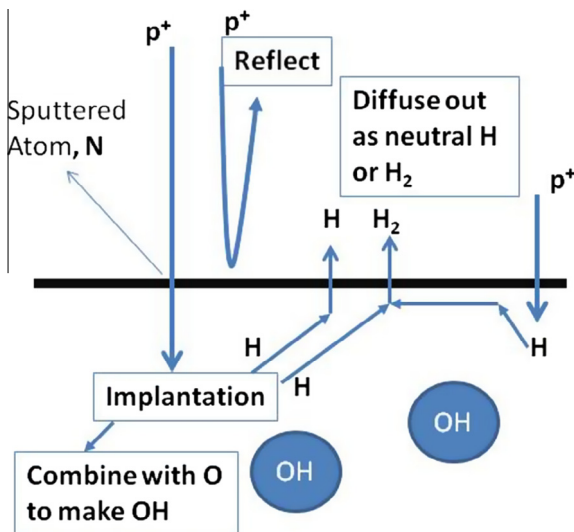

Fig. 1. Illustration of the possible surface interaction pathways for an implanted solar wind proton.
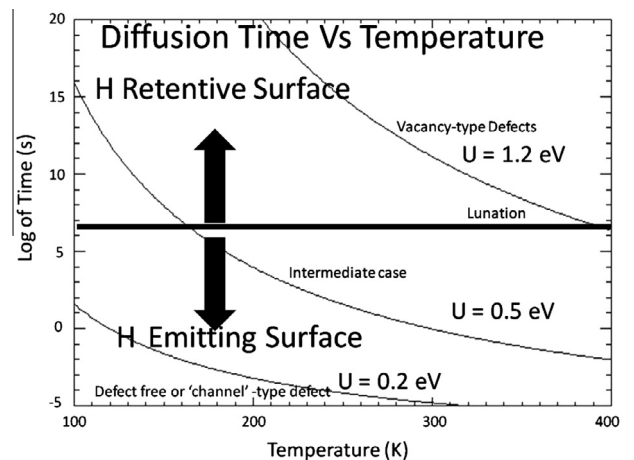

Fig. 2. Diffusion time as a function of temperature for a family of activation energies, U.